New atomic data for Kr XXXV useful in fusion plasma

Sunny Aggarwal†, Jagjit Singh, and Man Mohan
Department of Physics and Astrophysics, University of Delhi, Delhi 110007, *India*

(Received 16 September 2012; revised manuscript received 27 September 2012)

Energy levels and emission line wavelengths of high-Z materials are useful for impurity diagnostics due to their potential application in the next generation fusion devices. For this purpose, we have calculated the fine structural energies of the 67 levels belonging to the $1s^2$, 1s2l, 1s3l, 1s4l, 1s5l, and 1s6l configurations of Kr XXXV using GRASP (general purpose relativistic atomic structure package) code. Additionally, we have reported the transition probabilities, oscillator strengths, line strengths, and transition wavelengths for some electric dipole (E1) transitions among these levels. We predict new energy levels and radiative rates, which have not been reported experimentally or theoretically, forming the basis for future experimental work.

Keywords: atomic data, general purpose relativistic atomic structure package (GRASP) code, transition probability

PACS: 32.70.Cs **DOI:** 10.1088/1674-1056/22/3/033201

1. Introduction

Reliable atomic data for Krypton ions is of crucial importance for the modelling of plasma in fusion reactors and also for diagnostic purposes. Also, energy levels and radiative rates of helium-like ions have been a hot topic of investigations during the last few decades. Many authors have carried out studies on a helium isoelectronic sequence both theoretically and experimentally.[1,2] In this context, we have calculated energy levels, transition wavelengths, oscillator strengths, transition probabilities, and line strengths for the electric dipole (E1) transitions of the He-like krypton.

A large number of contributions have been made already, both experimentally and theoretically, regarding the atomic properties of He-like krypton, which is a clear indication of its importance in atomic physics and astrophysics.[3–6] Cheng[7] calculated the level energies for the 1s2l configuration, which were revised by Cheng and Chen.[8] Drake[9] also calculated the fine structural energies for the 1s3l configurations, while the energies for 1s4l and 1s5l levels were calculated by Vainshtein and Safronova,[10] where all levels were adjusted to the values at lower n of Drake.[9] They have also calculated the transition wavelengths for the 1s2s–2s2p, 1s2p–$2s^2$, and 1s2p–$2p^2$ transitions to explain the 2s2p, $2s^2$, and $2p^2$ levels. Furthermore, Widmann *et al*.[11] obtained four Kr XXXV lines using EBIT as their line source, whose uncertainty in measurement were 0.000026–0.000030 Å. Martin *et al*.[12] also obtained two lines using beam foil spectroscopy with uncertainties of 0.03 and 0.2 Å, respectively, which have also been measured by some other authors.[13–16] Natarajan A and Natarajan L[5] calculated the energies and electric dipole rates of k_β X-ray from $1s3p(^3P_1,^1P_1)$–$1s^2(^1S_0)$ transition for some He-like ions (including Kr XXXV). Griffin and Balance[4] calculated the fine structural energies of the lowest 49 levels of He-like krypton using the $\boldsymbol{R}$-matrix method. Recently, Zhang *et al*.[3] calculated the transition wavelengths, transition probabilities, line strengths, and oscillator strengths for some Kr ions (including He-like Krypton).

Energy levels for He-like krypton (Kr XXXV) have been compiled by the National Institute of Standards and Technology (NIST) and are available at their website http://www.nist.gov/pml/data/asd.cfm. In this paper, we have presented energy levels and radiative rates for some electric dipole transitions among the lowest 67 fine-structure levels of Kr XXXV, which belongs to $1s^2$, 1s2l, 1s3l, 1s4l, 1s5l, and 1s6l configurations. For our calculations, we have employed the fully relativistic general purpose relativistic atomic structure package (GRASP) code, originally developed by Grant *et al*.[17] and revised by Norrington to calculate radiative rates and energy levels. The GRASP code is a fully relativistic code and is based on the jj coupling scheme. In the present calculations, all the orbitals were simultaneously optimized on the average energy of all the configurations by using the option of an extended energy level (EAL). This procedure produces a compromise set of orbitals describing closely lying states with moderate accuracy. Firstly, zero-order Coulomb eigenvectors and energy levels have been calculated. Then, Breit interaction is added to the Hamiltonian and a further diagonalization in the configuration basis produces Breit-corrected eigenvectors and energy levels. Finally, quantum elctrodynamics (QED) effects (vacuum polarization and lamb shift) were estimated and corrected.

2. Energy levels

The $1s^2$, 1s2l, 1s3l, 1s4l, 1s5l, and 1s6l configurations of He-like Krypton give rise to 67 fine-structure energy levels, as listed in Table 1. Here, we present the calculated level energies via GRASP1 (without inclusion of Breit and QED effects) and GRASP2 (with the inclusion of Breit and QED effects).

†Corresponding author. E-mail: sunny.kmc87@gmail.com

© 2013 Chinese Physical Society and IOP Publishing Ltd

Table 1. Energy level (in Ry.) of the 67 first levels of Kr XXXV.

Index	Con.	Level	J	NIST	GRASP1	GRASP2	Ref. [4]
1	$1s^2$	^{1}S	0	0	0	0	0
2	1s2s	^{3}S	1	953.961461	955.676831	953.68979	955.686
3	1s2p	^{3}P^o	0	957.213955	958.612274	956.959939	958.62
4	1s2s	^{1}S	0	957.43640	958.961415	957.221378	958.97
5	1s2p	^{3}P^o	1	957.405686	959.201549	957.151848	959.21
6	1s2p	^{3}P^o	2	962.165052	963.977976	961.906094	963.986
7	1s2p	^{1}P^o	1	963.898464	965.680895	963.653884	965.69
8	1s3s	^{3}S	1	1131.5722	1133.37765	1131.31008	1133.387
9	1s3p	^{3}P^o	0	1132.4662	1134.18926	1132.20865	1134.198
10	1s3s	^{1}S	0	1132.504	1134.24376	1132.24788	1134.253
11	1s3p	^{3}P^o	1	1132.5190	1134.35026	1132.26254	1134.359
12	1s3p	^{3}P^o	2	1133.9379	1135.7757	1133.68099	1135.785
13	1s3d	^{3}D	1	1134.3990	1136.2162	1134.13942	1136.225
14	1s3d	^{3}D	2	1134.3735	1136.22746	1134.11451	1136.237
15	1s3p	^{1}P^o	1	1134.4136	1136.23751	1134.1611	1136.247
16	1s3d	^{3}D	3	1134.8665	1136.71564	1134.60596	1136.725
17	1s3d	^{1}D	2	1134.9066	1136.73391	1134.64621	1136.743
18	1s4s	^{3}S	1	1193.1101	1194.94502	1192.85808	1194.954
19	1s4p	^{3}P^o	0	1193.4819	1195.27873	1193.2267	1195.288
20	1s4s	^{1}S	0	1193.4937	1195.29627	1193.23945	1195.306
21	1s4p	^{3}P^o	1	1193.5065	1195.34472	1193.24911	1195.354
22	1s4p	^{3}P^o	2	1194.1034	1195.94617	1193.84758	1195.955
23	1s4d	^{3}D	1	1194.297	1196.12704	1194.03649	1196.136
24	1s4d	^{3}D	2	1194.2865	1196.13305	1194.02726	1196.142
25	1s4p	^{1}P^o	1	1194.3030	1196.13531	1194.04503	1196.145
26	1s4d	^{3}D	3	1194.4952	1196.33808	1194.23354	1196.347
27	1s4d	^{1}D	2	1194.5116	1196.34802	1194.25269	1196.357
28	1s4f	^{3}F^o	2	–	1196.34898	1194.2521	1196.358
29	1s4f	^{3}F^o	3	–	1196.34907	1194.24529	1196.358
30	1s4f	^{3}F^o	4	–	1196.45357	1194.35044	1196.463
31	1s4f	^{1}F^o	3	–	1196.4537	1194.35565	1196.463
32	1s5s	^{3}S	1	1221.4213	1223.26147	1221.16768	1223.271
33	1s5p	^{3}P^o	0	–	1223.4301	1221.35373	1223.439
34	1s5s	^{1}S	0	1221.6164	1223.43825	1221.35994	1223.448
35	1s5p	^{3}P^o	1	1221.6227	1223.46344	1221.36517	1223.473
36	1s5p	^{3}P^o	2	1221.9280	1223.77106	1221.67127	1223.78
37	1s5d	^{3}D	1	–	1223.86246	1221.76689	1223.872
38	1s5d	^{3}D	2	–	1223.8658	1221.76244	1223.875
39	1s5p	^{1}P^o	1	1222.0310	1223.86669	1221.77128	1223.876
40	1s5d	^{3}D	3	–	1223.97053	1221.86778	1223.98
41	1s5d	^{1}D	2	–	1223.97612	1221.87806	1223.985
42	1s5f	^{3}F^o	2	–	1223.97664	1221.8778	1223.986
43	1s5f	^{3}F^o	3	–	1223.97671	1221.87433	1223.986
44	1s5f	^{3}F^o	4	–	1224.03023	1221.92818	1224.04
45	1s5f	^{1}F^o	3	–	1224.03034	1221.93089	1224.04
46	1s5g	^{3}G	3	–	1224.03036	1221.93058	1224.04
47	1s5g	^{3}G	4	–	1224.03036	1221.92855	1224.04
48	1s5g	^{3}G	5	–	1224.06242	1221.96078	1224.072
49	1s5g	^{1}G	4	–	1224.06242	1221.96238	1224.072
50	1s6s	^{3}S	1	–	1238.57671	1236.47991	–
51	1s6p	^{3}P^o	0	–	1238.67352	1236.58662	–
52	1s6s	^{1}S	0	–	1238.67837	1236.59064	–
53	1s6p	^{3}P^o	1	–	1238.6927	1236.59328	–
54	1s6p	^{3}P^o	2	–	1238.87048	1236.7702	–
55	1s6d	^{3}D	1	–	1238.92296	1236.82515	–
56	1s6d	^{3}D	2	–	1238.92497	1236.82266	–
57	1s6p	^{1}P^o	1	–	1238.92559	1236.82789	–
58	1s6d	^{3}D	3	–	1238.9855	1236.88352	–
59	1s6d	^{1}D	2	–	1238.98888	1236.88961	–
60	1s6f	^{3}F^o	2	–	1238.98919	1236.88947	–
61	1s6f	^{3}F^o	3	–	1238.98924	1236.88748	–
62	1s6f	^{3}F^o	4	–	1239.02021	1236.91864	–
63	1s6f	^{1}F^o	3	–	1239.02029	1236.92022	–
64	1s6g	^{3}G	3	–	1239.0203	1236.92004	–
65	1s6g	^{3}G	4	–	1239.0203	1236.91887	–
66	1s6g	^{3}G	5	–	1239.03886	1236.93753	–
67	1s6g	^{1}G	4	–	1239.03886	1236.93846	–

Moreover, we have compared our results with the critically evaluated data compiled by NIST,[18] which are commonly used as reference set for atomic results. In Table 1, we have also presented the results of Griffin and Balance[4] for comparison. As can be seen in Table 1, we have presented the results for many spectral lines, which are not listed in the NIST table. Data for higher levels corresponding to 1s6l (l=0–5) are obtained for the first time. Therefore, the present calculations will enrich the database of Kr XXXV and can be used in modelling applications.

From Table 1, one can see that our results obtained neglecting Breit and QED effects (GRASP1) are higher than the NIST values by ~ 2 Ry. Additionally, the ordering slightly differs in a few instances. For instance, the ordering for levels 4/5, 13/14, and 23/24 is different from data listed by the NIST, but the energy differences between these levels are very small. However, with the inclusion of Breit and QED effects (GRASP2), our results are lower than the NIST values by ~ 0.25 Ry. Furthermore, the ordering of our GRASP2 results are as same as that of the NIST results. This was expected as He-like Krypton inner shell radial functions are altered sufficiently due to relativistic effects. It is safer to use a relativistic atomic structure theory rather than a non-relativistic one. Therefore, our GRASP2 results are much closer to the NIST listings than the GRASP1 results, as we have included the Breit and QED effects in GRASP2. Finally, we can state that there is no major discrepancy between our theoretical levels and the NIST listing levels of He-like Krypton. We believe that our energy levels from the GRASP2 calculations can be used in modelling applications.

Now, we would like to discuss the accuracy of our calculated results. To find accurate and reliable energy levels, we have calculated the results using GRASP1 and GRASP2. The GRASP1 energy levels are in good agreement with that of Griffin and Balance,[4] while our GRASP2 results are very close to the NIST listings ($\sim 0.03\%$) for all the configurations. This is because they[4] did not include Breit and QED effects, nor we these included by us in GRASP1 calculations. The disagreement between our calculated GRASP1 energies and the NIST energies of all the presented configurations is about 0.2%. This is due to mixing present in these levels with the other levels in our calculations. Based on these and other comparisons, we can state that our GRASP2 results are probably the best.

Figure 1 shows the ratio of energy levels calculated in this work to values compiled by the NIST as a function of our calculated GARSP1 energy. Similarly, figure 2 shows the ratio of energy levels calculated in this work (relative to the ground state, in Ry.) to values compiled by the NIST as a function of our calculated GARSP2 energy. From Figs. 1 and 2, one can see that our GRASP2 results are much closer to the NIST data than the GARSP1 ones.

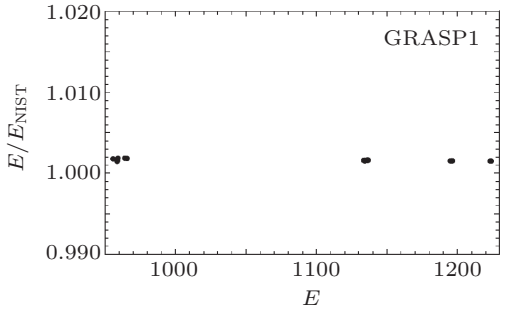


Fig. 1. Ratio of energy levels calculated in this work (E) (relative to the ground state, in Ry.) to values compiled by the NIST ($E_{\rm NIST}$) as a function of our calculated GARSP1 energy.

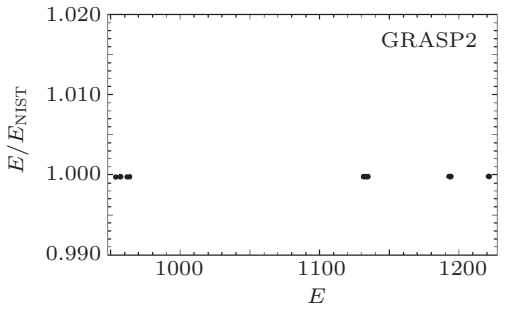


Fig. 2. Ratio of energy levels (E) calculated in this work (relative to the ground state, in Ry.) to values compiled by the NIST ($E_{\rm NIST}$) as a function of our calculated GARSP2 energy.

3. Radiative rates

Oscillator strengths or transition probabilities are the atomic structure constants that characterize the strength of radiative transitions, i.e., spectral lines, between two levels of an atom or atomic ion. We can connect the absorption oscillator strength (f_{ij}) with the transition probabilities A_{ji} (in s^{-1}) for a transition $i \rightarrow j$, described by the following expression:

$$f_{ij} = \frac{mc\omega_j}{8\pi^2 e^2 \omega_i} \lambda_{ji}^2 A_{ji}. \tag{1a}$$

After using the value of $mc/(8\pi^2 e^2) = 1.49 \times 10^{-16}$, equation (1a) becomes

$$f_{ij} = 1.49 \times 10^{-16} \frac{\omega_j}{\omega_i} \lambda_{ji}^2 A_{ji}, \tag{1b}$$

where c is the velocity of light, e and m are the electron charge and mass, respectively. Also, λ_{ji}^2 is the transition wavelength (in Å), and ω_i and ω_j are the statistical weights of the lower and upper levels, respectively. We may also define another relevant parameter, line strength, as

$$S = S(i,j) = S(j,i) = \left|R_{ij}\right|^2, \tag{2a}$$

$$R_{ij} = \left|\left\langle \psi_j \left| P \right| \psi_i \right\rangle\right|, \tag{2b}$$

where ψ_i and ψ_j represent the initial and final state wavefunctions, and R_{ij} represent the transition matrix element of the

appropriate multipole operator P. We can correlate the dimensionless oscillator strength f_{ij} and line strength (in a.u.) by the following equations. For the electric dipole (E1) transitions,

$$A_{ji} = \frac{2.0261 \times 10^{18}}{\omega_j \lambda_{ji}^3} S_{\mathrm{E1}}, \quad f_{ij} = \frac{303.75}{\lambda_{ji} \omega_i} S_{\mathrm{E1}}. \tag{3}$$

For the magnetic dipole (M1) transitions,

$$A_{ji} = \frac{2.6974 \times 10^{13}}{\omega_j \lambda_{ji}^3} S_{\mathrm{M1}}, \quad f_{ij} = \frac{4.044 \times 10^{-3}}{\lambda_{ji} \omega_i} S_{\mathrm{M1}}. \tag{4}$$

For the electric quadrupole (E2) transitions,

$$A_{ji} = \frac{1.1199 \times 10^{18}}{\omega_j \lambda_{ji}^5} S_{\mathrm{E2}}, \quad f_{ij} = \frac{167.89}{\lambda_{ji}^3 \omega_i} S_{\mathrm{E2}}. \tag{5}$$

For the magnetic quadrupole (M2) transitions,

$$A_{ji} = \frac{1.4910 \times 10^{13}}{\omega_j \lambda_{ji}^5} S_{\mathrm{M2}}, \quad f_{ij} = \frac{2.236 \times 10^{-3}}{\lambda_{ji}^3 \omega_i} S_{\mathrm{M2}}. \tag{6}$$

We have presented the transition wavelengths (in Å), transition probabilities (A_{ji} in s^{-1}), oscillator strengths (f_{ij}, dimensionless), and line strength (S in a.u) obtained with the GRASP code for some electric dipole (E1) transitions among the 67 levels of Kr XXXV in Table 2. The indices used to represent the lower and upper level of a transition which has already been defined in Table 1. Ratios between velocity and length forms for electric dipole transitions are also provided. The difference between both forms for many strong E1-type transitions ($f \geq 0.1$) does not exceed 4%. For 70% of the electric dipole transitions, the values of length and velocity forms are found to be equal, indicating that our transition characteristics are quite accurate and reliable. However, for 1.2% of strong transitions ($f \geq 0.1$), the two forms f-value differ by up to an order of magnitude. Additionally, the difference between the length and velocity forms for some weaker transitions ($f < 0.1$) can sometimes be large, such as transition 4–7. All such weak transitions sensitive to the mixing coefficients do not affect the overall accuracy of the calculations. Additionally, because their transition energy is very small, hence a slight variation in ΔE has a considerable effect on the values of A. We have also presented the wavelength compiled by NIST and calculated by Saloman[18] for comparison. One can see from Table 2 that the wavelengths for all transitions agree with the NIST data. The largest differences for the wavelengths are predicted for transitions between energy levels, which show the largest discrepancies from NIST energies. In Table 3, we have compared our calculated A-value with some previously published values. It can be seen from Table 3 that our calculated results are in excellent agreement with the other results, giving its credit to the accuracy of our results.

Table 2. Transition wavelengths (λ_{ij} in Å), transition probabilities (A_{ji} in s^{-1}), oscillator strengths (f_{ij}), and line strength (S in a.u.), and Vel/Len ratios for E1 transitions.

i	j	λ_{ij}(NIST)	λ_{ij}	A_{ji}	f_{ij}	S	Vel/Len
1	5	0.95180	0.95207	3.944×10^{14}	1.608×10^{-1}	5.039×10^{-4}	0.990
1	7	0.94538	0.94564	1.529×10^{15}	6.148×10^{-1}	1.914×10^{-3}	0.990
1	11	0.804637	0.80482	1.099×10^{14}	3.203×10^{-2}	8.486×10^{-5}	0.980
1	15	0.803294	0.80348	4.196×10^{14}	1.218×10^{-1}	3.223×10^{-4}	0.980
1	21	0.763521	0.76369	4.515×10^{13}	1.184×10^{-2}	2.978×10^{-5}	0.990
1	25	0.763012	0.76318	1.723×10^{14}	4.513×10^{-2}	1.134×10^{-4}	0.980
1	35	0.745948	0.74611	2.169×10^{13}	5.431×10^{-3}	1.334×10^{-5}	1.00
1	39	0.745699	0.7.4586	8.312×10^{13}	2.080×10^{-2}	5.107×10^{-5}	1.00
1	53	–	0.73692	1.250×10^{13}	3.054×10^{-3}	7.409×10^{-6}	1.00
1	57	–	0.73678	4.809×10^{13}	1.174×10^{-2}	2.848×10^{-5}	1.00
2	3	279.8	278.66	6.441×10^{8}	2.500×10^{-3}	6.879×10^{-3}	1.40
2	5	264.6	263.22	6.126×10^{8}	6.363×10^{-3}	1.654×10^{-2}	1.50
2	6	111.11	110.91	1.055×10^{10}	3.242×10^{-2}	3.551×10^{-2}	1.20
2	7	91.7	91.456	3.808×10^{9}	4.775×10^{-3}	4.313×10^{-3}	1.10
2	9	–	5.1046	3.495×10^{13}	4.551×10^{-2}	2.295×10^{-3}	1.00
2	11	5.1035	5.1031	2.759×10^{13}	1.077×10^{-1}	5.429×10^{-3}	1.00
2	12	5.0633	5.0629	3.279×10^{13}	2.100×10^{-1}	1.050×10^{-2}	1.00
2	15	–	5.0494	6.695×10^{12}	2.559×10^{-2}	1.276×10^{-3}	1.00
2	19	–	3.8043	1.502×10^{13}	1.086×10^{-2}	4.081×10^{-4}	1.00
2	21	3.80416	3.8040	1.182×10^{13}	2.565×10^{-2}	9.636×10^{-4}	1.00
2	22	3.79470	3.7945	1.438×10^{13}	5.174×10^{-2}	1.939×10^{-3}	1.00
2	25	–	3.7914	2.998×10^{12}	6.462×10^{-3}	2.420×10^{-4}	1.00
2	28	–	3.7881	9.234×10^{5}	3.311×10^{-9}	1.239×10^{-10}	0.810
2	33	–	3.4045	7.612×10^{12}	4.409×10^{-3}	1.483×10^{-4}	1.00
2	35	3.40455	3.4044	5.985×10^{12}	1.040×10^{-2}	3.497×10^{-4}	1.00

Table 2. (*Continued*).

i	j	λ_{ij}(NIST)	λ_{ij}	A_{ji}	f_{ij}	S	Vel/Len
2	36	3.40067	3.4005	7.340×10^{12}	2.121×10^{-2}	7.122×10^{-4}	1.00
2	39	–	3.3992	1.545×10^{12}	2.675×10^{-3}	8.982×10^{-5}	1.00
2	42	–	3.3979	1.132×10^{6}	3.265×10^{-9}	1.096×10^{-10}	0.610
2	51	–	3.2212	4.341×10^{12}	2.251×10^{-3}	7.160×10^{-5}	1.00
2	53	–	3.2211	3.411×10^{12}	5.306×10^{-3}	1.688×10^{-4}	1.00
2	54	–	3.2191	4.191×10^{12}	1.085×10^{-2}	3.450×10^{-4}	1.00
2	57	–	3.2185	8.865×10^{11}	1.377×10^{-3}	4.376×10^{-5}	1.00
2	60	–	3.2178	1.005×10^{6}	2.600×10^{-9}	8.263×10^{-11}	0.510
3	8	–	5.2267	1.235×10^{12}	1.518×10^{-2}	2.611×10^{-4}	1.00
3	13	5.1430	5.1432	5.578×10^{13}	6.637×10^{-1}	1.124×10^{-2}	1.00
3	18	–	3.8630	4.947×10^{11}	3.320×10^{-3}	4.223×10^{-5}	1.00
3	23	3.84365	3.8438	1.821×10^{13}	1.210×10^{-1}	1.532×10^{-3}	1.00
3	32	–	3.4491	2.430×10^{11}	1.300×10^{-3}	1.476×10^{-5}	1.00
3	37	–	3.4413	8.383×10^{12}	4.465×10^{-2}	5.058×10^{-4}	1.00
3	50	–	3.2601	1.357×10^{11}	6.484×10^{-4}	6.959×10^{-6}	1.00
3	55	–	3.2561	4.589×10^{12}	2.188×10^{-2}	2.345×10^{-4}	1.00
5	4	–	1.3106×10^{4}	3.710×10^{3}	3.184×10^{-5}	4.122×10^{-3}	130
4	7	141	141.67	4.071×10^{9}	3.674×10^{-2}	1.714×10^{-2}	0.760
4	11	–	5.2060	7.442×10^{12}	9.071×10^{-2}	1.555×10^{-3}	1.00
4	15	5.1486	5.1502	2.617×10^{13}	3.122×10^{-1}	5.293×10^{-3}	1.00
4	21	–	3.8609	3.268×10^{12}	2.191×10^{-2}	2.785×10^{-4}	0.990
4	25	3.84717	3.8479	1.167×10^{13}	7.773×10^{-2}	9.847×10^{-4}	0.990
4	35	–	3.4499	1.720×10^{12}	9.209×10^{-3}	1.046×10^{-4}	0.970
4	39	3.44401	3.4446	6.198×10^{12}	3.308×10^{-2}	3.751×10^{-4}	0.960
4	53	–	3.2619	1.031×10^{12}	4.934×10^{-3}	5.298×10^{-5}	0.940
4	57	–	3.2591	3.759×10^{12}	1.796×10^{-2}	1.927×10^{-4}	0.930
5	8	5.2322	5.2324	2.882×10^{12}	1.183×10^{-2}	6.112×10^{-4}	1.00
5	10	–	5.2044	2.060×10^{12}	2.788×10^{-3}	1.433×10^{-4}	0.950
5	13	5.1486	5.1488	3.345×10^{13}	1.330×10^{-1}	6.761×10^{-3}	1.00
5	14	5.1493	5.1495	7.873×10^{13}	5.217×10^{-1}	2.653×10^{-2}	1.00
5	17	–	5.1341	1.558×10^{12}	1.026×10^{-2}	5.203×10^{-4}	1.00
5	18	3.86614	3.8661	1.144×10^{12}	2.564×10^{-3}	9.788×10^{-5}	1.00
5	20	–	3.8599	8.849×10^{11}	6.588×10^{-4}	2.512×10^{-5}	0.890
5	23	3.84676	3.8469	1.091×10^{13}	2.421×10^{-2}	9.197×10^{-4}	1.00
5	24	3.84694	3.8471	2.573×10^{13}	9.515×10^{-2}	3.615×10^{-3}	1.00
5	27	–	3.8434	4.575×10^{11}	1.688×10^{-3}	6.409×10^{-5}	1.00
5	32	3.45156	3.4516	5.538×10^{11}	9.892×10^{-4}	3.372×10^{-5}	1.10
5	34	–	3.4491	4.812×10^{11}	2.861×10^{-4}	9.744×10^{-6}	0.820
5	37	–	3.4438	5.014×10^{12}	8.915×10^{-3}	3.032×10^{-4}	1.00
5	38	–	3.4438	1.186×10^{13}	3.515×10^{-2}	1.195×10^{-3}	1.00
5	41	–	3.4423	1.957×10^{11}	5.793×10^{-4}	1.969×10^{-5}	1.00
5	50	–	3.2624	3.031×10^{11}	4.837×10^{-4}	1.558×10^{-5}	1.10
5	52	–	3.2611	3.091×10^{11}	1.643×10^{-4}	5.290×10^{-6}	0.740
5	55	–	3.2583	2.741×10^{12}	4.363×10^{-3}	1.404×10^{-4}	1.00
5	56	–	3.2584	6.502×10^{12}	1.725×10^{-2}	5.551×10^{-4}	1.00
5	59	–	3.2576	1.006×10^{11}	2.666×10^{-4}	8.578×10^{-6}	1.10
6	8	5.3792	5.3793	6.776×10^{12}	1.764×10^{-2}	1.562×10^{-3}	1.00
6	13	–	5.2909	2.699×10^{12}	6.796×10^{-3}	5.919×10^{-4}	1.00
6	14	5.2917	5.2917	1.512×10^{13}	6.347×10^{-2}	5.528×10^{-3}	1.00
6	16	5.2765	5.2766	9.763×10^{13}	5.706×10^{-1}	4.956×10^{-2}	1.00
6	17	–	5.2754	9.274×10^{12}	3.869×10^{-2}	3.360×10^{-3}	1.00
6	18	3.94582	3.9457	2.666×10^{12}	3.734×10^{-3}	2.425×10^{-4}	1.00
6	23	–	3.9257	8.594×10^{11}	1.191×10^{-3}	7.698×10^{-5}	1.00
6	24	3.92582	3.9259	4.867×10^{12}	1.125×10^{-2}	7.267×10^{-4}	1.00
6	26	3.92229	3.9224	3.143×10^{13}	1.015×10^{-1}	6.552×10^{-3}	1.00
6	27	–	3.9220	2.934×10^{12}	6.767×10^{-3}	4.369×10^{-4}	1.00
6	32	3.51493	3.5149	1.284×10^{12}	1.427×10^{-3}	8.256×10^{-5}	1.10
6	37	–	3.5068	3.916×10^{11}	4.332×10^{-4}	2.501×10^{-5}	1.00
6	38	–	3.5068	2.224×10^{12}	4.101×10^{-3}	2.367×10^{-4}	1.00

Table 2. (*Continued*).

i	j	λ_{ij}(NIST)	λ_{ij}	A_{ji}	f_{ij}	S	Vel/Len
6	40	–	3.5054	1.436×10^{13}	3.705×10^{-2}	2.138×10^{-3}	1.00
6	41	–	3.5053	1.332×10^{12}	2.453×10^{-3}	1.415×10^{-4}	1.00
6	46	–	3.5046	1.066×10^{4}	2.749×10^{-11}	1.586×10^{-12}	1.90
6	50	–	3.3189	6.978×10^{11}	6.914×10^{-4}	3.777×10^{-5}	1.10
6	55	–	3.3147	2.135×10^{11}	2.110×10^{-4}	1.151×10^{-5}	1.00
6	56	–	3.3147	1.211×10^{12}	1.995×10^{-3}	1.088×10^{-4}	1.00
6	58	–	3.3140	7.820×10^{12}	1.803×10^{-2}	9.834×10^{-4}	1.00
6	59	–	3.3139	7.225×10^{11}	1.190×10^{-3}	6.489×10^{-5}	1.00
6	64	–	3.3136	9.546×10^{3}	2.200×10^{-11}	1.200×10^{-12}	2.40
7	8	–	5.4354	8.403×10^{11}	3.722×10^{-3}	1.998×10^{-4}	1.00
7	10	5.4047	5.4051	9.622×10^{12}	1.405×10^{-2}	7.499×10^{-4}	0.950
7	13	–	5.3452	8.059×10^{12}	3.452×10^{-2}	1.822×10^{-3}	1.00
7	14	–	5.3459	5.847×10^{12}	4.176×10^{-2}	2.205×10^{-3}	1.00
7	17	5.3288	5.3293	8.603×10^{13}	6.105×10^{-1}	3.213×10^{-2}	1.00
7	18	–	3.9758	3.322×10^{11}	7.872×10^{-4}	3.091×10^{-5}	1.00
7	20	3.96901	3.9692	4.090×10^{12}	3.220×10^{-3}	1.262×10^{-4}	0.890
7	23	–	3.9555	2.547×10^{12}	5.974×10^{-3}	2.334×10^{-4}	1.00
7	24	–	3.9556	1.762×10^{12}	6.889×10^{-3}	2.691×10^{-4}	0.990
7	27	3.95150	3.9518	2.768×10^{13}	1.080×10^{-1}	4.216×10^{-3}	1.00
7	32	–	3.5387	1.618×10^{11}	3.037×10^{-4}	1.061×10^{-5}	1.00
7	34	3.53591	3.5361	2.221×10^{12}	1.388×10^{-3}	4.847×10^{-5}	0.820
7	37	–	3.5305	1.157×10^{12}	2.161×10^{-3}	7.536×10^{-5}	1.00
7	38	–	3.5306	7.996×10^{11}	2.490×10^{-3}	8.684×10^{-5}	0.970
7	41	–	3.5290	1.275×10^{13}	3.968×10^{-2}	1.383×10^{-3}	0.990
7	50	–	3.3401	8.882×10^{10}	1.486×10^{-4}	4.900×10^{-6}	1.10
7	52	–	3.3388	1.436×10^{12}	7.998×10^{-4}	2.637×10^{-5}	0.730
7	55	–	3.3359	6.273×10^{11}	1.047×10^{-3}	3.448×10^{-5}	1.00
7	56	–	3.3359	4.436×10^{11}	1.233×10^{-3}	4.063×10^{-5}	0.930
7	59	–	3.3351	7.024×10^{12}	1.952×10^{-2}	6.430×10^{-4}	0.980

Table 3. Comparison of transition probability (s^{-1}) calculated in this work with data from several other works.

Transition	This work	Ref. [4]	Other works
$1s^2\ ^1S_0$–$1s2p\ ^3P_1$	3.944×10^{14}	3.95×10^{14}	3.9170×10^{14} a)
			3.8261×10^{14} a)
			1.11×10^{14} b)
$1s^2\ ^1S_0$–$1s2p\ ^1P_1$	1.529×10^{15}	1.53×10^{15}	1.5057×10^{15} a)
			1.4906×10^{15} a)
			4.38×10^{14} b)
$1s^2\ ^1S_0$–$1s3p\ ^3P_1$	1.099×10^{14}	1.10×10^{14}	
$1s^2\ ^1S_0$–$1s3p\ ^1P_1$	4.196×10^{14}	4.21×10^{14}	
$1s^2\ ^1S_0$–$1s4p\ ^3P_1$	4.515×10^{13}	4.50×10^{13}	
$1s^2\ ^1S_0$–$1s4p\ ^1P_1$	1.723×10^{14}	1.72×10^{14}	
$1s^2\ ^1S_0$–$1s5p\ ^3P_1$	2.169×10^{13}	2.15×10^{13}	
$1s^2\ ^1S_0$–$1s5p\ ^1P_1$	8.312×10^{13}	8.27×10^{13}	

a) Ref. [3], b) Ref. [5].

The ratios between length and velocity forms are provided for electric dipole (E1) transitions to provide an additional indicator of the accuracy of our MCDF results. The length form is used for electric transitions, as they are less sensitive to the accuracy of wavefunction compared with results obtained in the velocity form of the transition operator, and we would normally recommend the length results. Moreover, in the dipole-length form, relativistic corrections are included automatically, but extra terms should be added to the gradient matrix element to restore the equivalence relationship between length and velocity forms. In those cases where the LS coupling scheme is good, the velocity form can be used only for allowed transitions but not for spin-forbidden transitions.[19]

4. Conclusions

In this paper, results for multiconfiguration Dirac–Fock energy levels, radiative rates, and oscillator strengths for all transitions have been computed for He-like Krypton (Kr XXXV). The 67 lowest energy levels have been presented. We have also presented the data compiled by NIST for comparison. Furthermore, results of radiative rates have been calculated for electric dipole (E1) transitions. Based on the comparisons made between the length and velocity forms of the oscillator strength, we can say that our radiative rates are accurate (better than 4%) for the majority of strong transitions. Good agreement between our energy levels and the radiative rates for Kr XXXV and the available NIST data reflects the quality

of the wavefunctions considered by us for the present calculations. We hope that our data will be useful in astrophysics, modeling of a variety of plasma, and other applications.

Acknowledgements

Sunny Aggarwal is grateful to U.G.C. (India) for granting a fellowship, and Man Mohan thanks D.S.T. (India), U.G.C. (INDIA), and University of Delhi for financial support.

References

[1] Lee P, Leiber A J, Pradhan A K and Xu Y 1986 *Phys. Rev. A* **34** 3210
[2] Mohan M, Aggarwal S, Singh J and Jha A K S (Communicated)
[3] Zhang L, Jiang G, Hao L and Deng B 2011 *Phys. Scr.* **83** 025302
[4] Griffin D C and Balance C P 2009 *J. Phys. B* **42** 235201
[5] Natarajan A and Natarajan L 2008 *JQSRT* **109** 2281
[6] Natarajan L and Natarajan A 2009 *Phys. Rev. A* **79** 062513
[7] Cheng K T 1996 private communication
[8] Cheng K T and Chen M H 2000 *Phys. Rev. A* **61** 044503
[9] Drake G W F 1985 (Unpublished)
[10] Vainshtein L A and Safronova U I 1985 (Unpublished)
[11] Widmann K, Beiersdorfer P, Decaux V and Bitter M 1996 *Phys. Rev. A* **53** 2200
[12] Martin S, Denis A, Buchet-Poulizac M C, Buchet J P and Désesquelles J 1990 *Phys. Rev. A* **42** 6570
[13] Indelicato P, Briand J P and Tavernier M 1986 *Z. Phys. D* **2** 249
[14] Briand J P, Indelicato P, Tavernier M, Gorceix O, Liesen D, Beyer H F, Liu B, Warczak A and Desclaux J P 1984 *Z. Phys. A* **318** 1
[15] Gould H and Marrus R 1976 *Plenum* **1** 305
[16] Büttner R, Kraus B, Nicolai M, Schartner K H, Folkmann F, Mokler P H and Möller G 1993 *AIP Conf. Proc.* **274** 423
[17] Grant I P, Mckenzie B J, Norrington P H, Mayers D F and Pyper N C 1980 *Comput. Phys. Commun.* **21** 207
[18] Saloman E B 2007 *J. Phys. Chem. Ref. Data* **36** 215
[19] Hibbert A 2004 *Phys. Scr.* **T112** 207